

# Resonant flow instability of MHD surface waves

W.J. Tirry<sup>\*1</sup>, V.M. Čadež<sup>1</sup>, R. Erdélyi<sup>2</sup>, and M. Goossens<sup>1</sup>

<sup>1</sup> Centre for Plasma-Astrophysics, K.U. Leuven, Celestijnenlaan 200 B, B-3001 Heverlee, Belgium

<sup>2</sup> School of Mathematical and Computational Sciences, Univ. St. Andrews, St. Andrews, KY16 9SS, Scotland, UK

Received 25 November 1997 / Accepted 19 January 1998

**Abstract.** We study the effect of velocity shear on the spectrum of MHD surface waves. A nonuniform intermediate region is taken into account, so that the surface wave can be subject to resonant absorption. In order to deal in a mathematically and also physically consistent manner with the resonant wave excitation, we analytically derive the dissipative solution around the resonant surface in resistive MHD. Using these analytical solutions in our eigenvalue code, the effect of the velocity shear on the damping rate of the surface wave can easily be investigated with limited numerical effort. The presence of the flow can both increase and decrease the efficiency of resonant absorption. We also show how the resonance can lead to instability of the global surface mode for a certain range of values for the velocity shear. The resonant flow instabilities, which are physically distinct from the nonresonant Kelvin-Helmholtz instabilities can occur for velocity shears significantly below the Kelvin-Helmholtz threshold. Although resonant absorption as dissipation mechanism is present, the amplitude of the surface mode grows in time. The resonant flow instability can be explained in terms of negative energy waves: to get an unstable negative energy wave, some dissipative process is required to ensure energy dissipation.

**Key words:** MHD – waves – Sun: corona – Sun: magnetic fields

---

## 1. Introduction

The solar atmosphere, from the photosphere to the corona, is a highly structured inhomogeneous medium, e.g. recent observations of X-ray emission from the solar corona by Yokoh (Shibata et al. 1992) have emphasized the complex, highly structured nature of the corona. Commonly observed features such as the photospheric flux tubes, coronal holes, coronal loops, magnetic arcades indicate the existence of pronounced local nonuniformities at their boundaries. Another key observation of the highly inhomogeneous solar atmosphere is the presence of steady flows. Bulk motions are observed along or nearly along the magnetic field lines which outline the magnetic structures

(Doyle et al. 1997). The nonuniformities are often in the form of transition layers that separate regions of larger extent with different, comparatively uniform physical characteristics.

In particular, these sharply structured interfaces can support magneto-acoustic surface waves, which may be classified as either fast or slow modes (Roberts 1981).

An important property of MHD waves in an inhomogeneous plasma is that a global wave motion can be in resonance with local oscillations of a specific magnetic surface. The resonance condition is that the frequency of the global motion should be equal to either the local Alfvén or the local cusp frequency of the magnetic surface. In this way energy is transferred from the large scale motion to oscillations which are highly localized to the neighbourhood of the Alfvén or cusp singular surface. In dissipative MHD this behaviour is mathematically recovered as eigenmodes which are exponentially damped in time. Due to their global character (oscillating with the same frequency throughout the plasma) these modes are called ‘global modes’. For ideal MHD such damped oscillations cannot be eigenmodes of the system, and for this reason they are often called ‘quasi-modes’ (see Tirry & Goossens 1996 and references therein). Since quasi-modes turn out to be global natural oscillations of the magnetic structures they will probably be most easily observed. It is therefore important to know how the frequencies of the quasi-modes are related to the distribution of the physical quantities and the geometry of the structure. For the same reason the quasi-mode plays a central role in the resonant absorption process as possible heating mechanism.

Since the work of Ionson (1978), resonant absorption of MHD surface modes has been recognized as a suitably efficient damping mechanism, and much recent work has been devoted to this process (Rae & Roberts 1982; Lee & Roberts 1986; Davila 1987; Hollweg & Yang 1988; Hollweg et al. 1990; Sakurai, Goossens & Hollweg 1991; Goossens, Ruderman & Hollweg 1995; Erdélyi & Goossens 1996). Except for the paper by Hollweg et al. (1990) and Erdélyi & Goossens (1996), these prior studies and many others of resonant absorption have assumed that there is no background velocity shear in the plasma. However in the paper by Hollweg et al., the authors introduced velocity shear and investigated its effects on the rate of resonant absorption of MHD waves supported by thin “surfaces” in an incompressible plasma. They found that the velocity shear can

---

Send offprint requests to: W.Tirry

\* Research Assistant of the F.W.O.-Vlaanderen

either increase or decrease the resonant absorption rate and that for certain values of the velocity shear the absorption rate goes to zero. In addition, they also found that there can be resonances which do not absorb energy from the surface wave but rather give energy back to it, leading to instabilities, even at velocity shear, which are below the threshold for the Kelvin-Helmholtz instability (Chandrasekhar 1961).

Ryutova (1988) has considered a closely related problem. She studied the propagation of kink waves along thin magnetic flux tubes in the presence of a homogeneous parallel flow outside of the tube. She was the first to introduce the concept of negative energy waves to solar physics and suggested that the resonant instability can be interpreted in terms of negative energy waves. However, according to Hollweg et al. (1990), her work contains an inconsistency.

Erdélyi & Goossens (1996) studied the p-mode resonant interaction with steady inhomogeneous flux tubes (sunspots) and found that for steady flows at around 10 percent of the local Alfvén speed, sunspots emitted energy. This phenomenon was again associated with negative energy waves.

Joarder et al. (1997) applied the concept of negative energy waves for simple homogeneous solar configurations. They showed that backward propagating waves found in these magnetic structures of the solar atmosphere are negative energy waves.

Ruderman & Goossens (1995) studied the stability of an MHD tangential discontinuity in an incompressible plasma where viscosity is taken into account at one side of the discontinuity. The instability, which occurs for velocity shears smaller than the threshold value for the onset of the Kelvin-Helmholtz instability, can be explained in terms of a negative energy wave which becomes unstable because of the presence of a dissipation mechanism (viscosity).

Since these instabilities may play a role in the development of turbulence in regions of strong velocity shear such as in the solar wind and the Earth's magnetosheath, but also, for example, in the interaction of p-modes with sunspots, the assumption of incompressibility has to be dropped in the spectral study.

In addition, in order to deal in a mathematically but also physically consistent manner with the resonant wave excitation (the singularity in the ideal MHD equations) in solving the eigenvalue problem for the MHD surface modes, we analytically derive the dissipative solution close to the resonant magnetic surface in resistive MHD.

Hence in this paper we consider the spectral problem of the MHD surface mode on a transitional nonuniform layer that separates two uniform regions, and in the presence of a velocity shear (discontinuity) in the background flow. The mass flow is assumed to be uniform in one of the uniform regions and in the transitional layer whereas the other uniform region is static.

By deriving the solution in resistive MHD analytically around the resonance, the effect of the velocity shear on the damping rate can easily be investigated and it clearly shows how and when the resonant instability occurs. In the presence of a background flow it can be anticipated that the damping of the MHD surface mode due to resonant wave transformation is

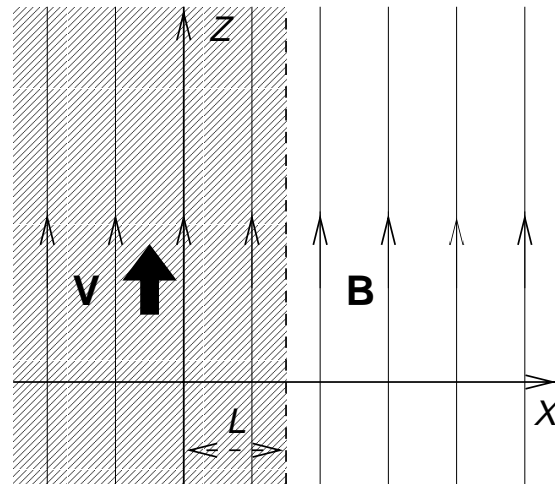


Fig. 1. A cartoon of the single interface in Cartesian coordinates.

altered, since the flow does not only Doppler shift the continuum frequencies but it also affects the energy of the eigenmodes. At the resonance the flow could drain energy away from the surface mode, which additionally increases the wave damping, but the flow could also be an energy source so that the surface mode gains energy and becomes unstable.

The paper is organized as follows. In Sect. 2 the stationary equilibrium configuration is described while in Sect. 3 the linearized MHD equations for small perturbations are discussed. The analytical dissipative solutions around the resonant surfaces are derived in Sect. 4. In Sect. 5 we shortly describe the numerical procedure for solving the spectrum of the MHD surface modes. The results are presented in Sect. 6 whereas the correspondence between the overstabilities and the negative energy waves is illustrated in Sect. 7. In Sect. 8 we give a summary.

## 2. The steady equilibrium state

We model a sharp interface by two semi-infinite homogeneous regions separated by a nonuniform layer. In the Cartesian coordinate system we use, the  $x$ -axis is along the direction of inhomogeneity, i.e. the equilibrium quantities depend on the  $x$ -coordinate only. The non-uniform layer extends from  $x = 0$  to  $x = L$  (see Fig. 1).

The magnetic field  $\mathbf{B}_0 = (0, 0, B_0)$  is assumed to be homogeneous throughout the whole space whereas the plasma flow, with velocity  $\mathbf{U}_0 = (0, 0, U_0(x))$  parallel to the magnetic field, exists only for  $x < L$ . In particular :

$$U_0(x) = \begin{cases} V, & x < L \\ 0, & x \geq L. \end{cases} \quad (1)$$

Thus the flow speed is discontinuous at  $x = L$ , while the other physical quantities such as density  $\rho_0(x)$  and temperature  $T_0(x)$  are assumed to behave smoothly through the nonuniform layer.

In our treatment we ignore gravity, so that the magnetohydrostatic equation is simply given by

$$\frac{d}{dx} \left( p_0 + \frac{B_0^2}{2\mu} \right) = 0.$$

This means that the thermal pressure  $p_0$  is uniform and the plasma  $\beta$  parameter constant

$$\beta \equiv \frac{p_0}{p_m} = \frac{2v_S^2}{\gamma v_A^2} = \text{const}, \quad (2)$$

where  $p_m \equiv B_0^2/(2\mu_0)$  while  $v_A^2(x) \equiv B_0^2/(\mu_0\rho_0(x))$  and  $v_S^2(x) \equiv \gamma p_0/\rho_0(x)$  are the squares of the Alfvén and the sound speed respectively.

The Alfvén speed is assumed to have a linear profile through the nonuniform layer and to be constant elsewhere :

$$v_A(x) = \begin{cases} v_{A1}, & x < 0 \\ v_{A1} - (v_{A1} - v_{A2})\frac{x}{L}, & 0 \leq x \leq L \\ v_{A2}, & x > L. \end{cases} \quad (3)$$

Since  $\beta$  is constant (2), the speed of sound is simply proportional to  $v_A(x)$  :

$$v_S(x) = \left(\frac{\gamma\beta}{2}\right)^{\frac{1}{2}} v_A(x).$$

We also introduce the cusp speed  $v_C(x)$  which is defined as

$$v_C(x) \equiv \frac{v_A v_S}{(v_A^2 + v_S^2)^{\frac{1}{2}}} = \frac{(\gamma\beta)^{\frac{1}{2}}}{(2 + \gamma\beta)^{\frac{1}{2}}} v_A(x).$$

Besides the plasma  $\beta$  parameter, the configuration is also characterized by the temperature ratio  $r_T \equiv T_2/T_1$ , which can be written in terms of the Alfvén speeds in the two homogeneous regions as

$$r_T = \frac{v_{A2}^2}{v_{A1}^2}. \quad (4)$$

According to the definition of the Alfvén speed and from (3) and (4) the density profile  $\rho_0(x)$  in the nonuniform layer takes the following form :

$$\rho_0(x) = \left(1 - \frac{1 - \sqrt{r_T}}{L}x\right)^{-2} \rho_0(0). \quad (5)$$

For the rest of the paper, length, speed, density and magnetic field strength are non-dimensionalized with respect to  $1/\sqrt{k_y^2 + k_z^2}$ ,  $v_{A2}$ ,  $\rho_0(L)$  and  $B_0$  respectively.  $k_y$  and  $k_z$  are the  $y$ - and  $z$ -component of the wave vector of the MHD surface mode on the sharp interface.

The unperturbed plasma is taken to be ideal because the dissipative effects can be neglected on the time scale of the MHD wave propagation.

### 3. The linearized MHD equations

In the presence of linear perturbations it is not any longer true that the plasma can be taken to be ideal everywhere. We shall see that dissipation cannot be ignored near the possible resonant points due to the local quasi-singular behaviour of the solutions. In our model we shall include the Ohmic heating as the only dissipation mechanism and exclude the effects of viscosity and thermal conduction.

The standard set of linearized MHD equations for a resistive plasma is

$$\begin{aligned} \frac{\partial \rho_1}{\partial t} + \nabla \cdot (\rho_0 \mathbf{v}_1 + \rho_1 \mathbf{v}_0) &= 0, \\ \rho_0 \left[ \frac{\partial \mathbf{v}_1}{\partial t} + (\mathbf{v}_0 \cdot \nabla) \mathbf{v}_1 + (\mathbf{v}_1 \cdot \nabla) \mathbf{v}_0 \right] + \rho_1 (\mathbf{v}_0 \cdot \nabla) \mathbf{v}_0 &= \\ -\nabla p_1 + \frac{1}{\mu_0} (\nabla \times \mathbf{B}_1) \times \mathbf{B}_0 + \frac{1}{\mu_0} (\nabla \times \mathbf{B}_0) \times \mathbf{B}_1, & \quad (6) \\ \frac{\partial \mathbf{B}_1}{\partial t} &= \nabla \times (\mathbf{v}_1 \times \mathbf{B}_0) + \nabla \times (\mathbf{v}_0 \times \mathbf{B}_1) + \eta \nabla^2 \mathbf{B}_1, \\ \rho_0 \left[ \frac{\partial \mathbf{T}_1}{\partial t} + \mathbf{v}_0 \cdot \nabla \mathbf{T}_1 \right] &= \\ -\rho_0 \mathbf{v}_1 \cdot \nabla T_0 - (\gamma - 1) \rho_0 T_0 \nabla \cdot \mathbf{v}_1, & \\ \frac{p_1}{p_0} &= \frac{\rho_1}{\rho_0} + \frac{T_1}{T_0}. \end{aligned}$$

As the equilibrium quantities depend on the  $x$ -coordinate only, the perturbed quantities  $f_1$  are Fourier analyzed with respect to  $y$ ,  $z$  and  $t$ . The amplitudes of the corresponding Fourier components remain  $x$ -dependent:

$$f_1(x, y, z, t) = f(x, k_y, k_z; \omega) \exp^{i(k_y y + k_z z - \omega t)}.$$

Because of the very high values of the magnetic Reynolds number, e.g. for the solar coronal conditions, the dissipation due to the finite electrical resistivity  $\eta$  can be ignored except in narrow layers of steep gradients (e.g. around resonances). Outside these dissipative layers the Eqs. (6) reduce to the following two coupled first order differential equations for the perturbations of the normal component of the Lagrangian displacement  $\xi_x$  and of the Eulerian perturbation of total pressure  $P$  :

$$D \frac{d\xi_x}{dx} = -C_1 P, \quad \frac{dP}{dx} = C_2 \xi_x \quad (7)$$

where

$$D = \rho_0 (v_S^2 + v_A^2) (\Omega^2 - \omega_C^2) (\Omega^2 - \omega_A^2),$$

$$C_1 = (\Omega^2 - \omega_A^2) (\Omega^2 - \omega_S^2) - \Omega^2 v_A^2 k_y^2,$$

$$C_2 = \rho_0 (\Omega^2 - \omega_A^2)$$

and

$$\begin{aligned} \Omega &= \omega - k_z V, \\ \omega_A &= v_A k_z, \quad \omega_S = v_s \sqrt{k_y^2 + k_z^2}, \quad \omega_C = v_C k_z. \end{aligned}$$

$C_1$  can be rewritten as

$$C_1 = (\Omega^2 - \omega_I^2) (\Omega^2 - \omega_{II}^2)$$

where  $\omega_I$  and  $\omega_{II}$  are known as the cut-off frequencies.

The inclusion of the equilibrium flow  $V$  causes only a replacement of the frequency  $\omega$  by the Doppler shifted frequency  $\Omega$  in the equations with respect to the static case. (see e.g. Goossens, Sakurai & Hollweg 1992).

The set of ordinary differential Eqs. (7) has mobile regular singularities at the positions  $x_A$  and/or  $x_C$  where  $D(x)$  vanishes:

$$\Omega = \pm\omega_A(x_A) \quad \text{and/or} \quad \Omega = \pm\omega_C(x_C).$$

or

$$\omega = k_z V \pm \omega_A(x_A) \quad \text{and/or} \quad \omega = k_z V \pm \omega_C(x_C) \quad (8)$$

As both  $\omega_A(x)$  and  $\omega_C(x)$  are functions of  $x$ , they define two continuous ranges of frequencies referred to as the Alfvén continuum and the slow continuum respectively. These continua are now Doppler shifted due to the presence of the flow as indicated by Eqs. (8).

From a physical point of view, the conditions (8) mean that the eigenmodes resonantly interact with one of the two continua and also with the flow. The interaction with the continua in the absence of the flow causes damping of the eigenmode due to resonant wave transformation and we talk about quasi-modes with complex eigenfrequency  $\omega = \omega_r + i\omega_i$  with  $\omega_i < 0$  in this case (Tirry & Goossens 1996 and references therein). If however a flow is present then it not only Doppler shifts the continuum frequencies but it can also affect the energy of the eigenmodes. At the resonance, the flow can namely drain energy away from the surface modes, which additionally increases the wave damping, but the flow can also be an energy source in which case the surface modes gain energy and become unstable, i.e.  $\omega_i > 0$ .

#### 4. The analytical solution around the resonance

In ideal MHD, the solutions diverge at the resonance points as defined by (8). To remove the singularity from the ideal MHD Eqs. (7) we include, for regions close to the resonances, the dissipative terms into the equations. The overall solutions for  $\xi_x$  and  $P$  are now obtained by solving the ideal Eqs. (7) outside the dissipative layers and the dissipative Eqs. (6) inside the layers with the requirement for continuous solutions at the boundaries of the layers. In the close vicinity of the resonant points, we can simplify the initial set of Eqs. (6) by reducing them first to a form analogous to (7) and then express the coefficients as linear functions of the distance  $s$  from the resonant point (see e.g. Erdélyi, Goossens & Ruderman 1995). Due to the resonant coupling in the presence of a background flow, the waves could lose or gain energy as pointed out in the previous section and therefore their eigenfrequencies are complex:  $\omega = \omega_r + i\omega_i$ . In the case of the Alfvén resonance at  $s \equiv x - x_A = 0$  the Eqs. (6) can be approximated in some interval  $[-s_A, +s_A]$  around the resonance, by the following set

$$\begin{aligned} & \left[ 2i\Omega_r\omega_i + s\Delta_A - i\Omega_r\eta\frac{d^2}{ds^2} \right] \frac{d\xi_x}{ds} \\ &= - \left[ (2i\Omega_r\omega_i + s\Delta_A)\frac{\omega_A^2 - \omega_S^2}{\rho_0 v_A^2 \omega_A^2} - \frac{k_y^2}{\rho_0} \right] P, \\ & \frac{dP}{ds} = \rho_0(2i\Omega_r\omega_i + s\Delta_A)\xi_x, \end{aligned} \quad (9)$$

where  $\Omega_r = \omega_r - k_z V = \pm\omega_A$ ,  $\Delta_A \equiv (d/ds)(\Omega^2 - \omega_A^2)$  and the coefficients are evaluated at  $s = 0$ . Also,  $|\omega_i| \ll |\omega_A|$  is assumed but this has to be checked a posteriori when the solutions are obtained. In the numerical code the resistivity  $\eta$  is assumed to be important only inside the narrow dissipative layer  $[-d_{\eta A}, +d_{\eta A}]$  whose half-thickness  $d_{\eta A}$  is evaluated in our calculations as  $d_{\eta A} \approx 5 \times \delta_A$  where

$$\delta_A = \left( \frac{\omega_A \eta}{|\Delta_A|} \right)^{\frac{1}{3}}$$

defines the length scale of the resonance layer as can be estimated from the first equation in (9).

In the Eqs. (9) the highest derivative term is multiplied with the electrical resistivity. Hence for very high Reynolds numbers, the Eqs. (9) represents a singular perturbation problem. Now it is convenient to introduce a new scaled variable  $\tau = s/\delta_A$ , which is of the order 1 in the dissipative layer. With this new variable the Eqs. (9) for  $\xi_x$  and  $P$  take the form:

$$\begin{aligned} & \left[ \frac{d^2}{d\tau^2} + i \operatorname{sign}(\Delta_A \Omega_r) \tau - \Lambda_A \right] \frac{d\xi_x}{d\tau} = - \left\{ -i \frac{\operatorname{sign}(\Omega_r) k_y^2}{\rho_0 |\Delta_A|} \right. \\ & \left. + \delta_A [-\Lambda_A + i \operatorname{sign}(\Delta_A \Omega_r) \tau] \frac{\omega_A^2 - \omega_S^2}{\rho_0 v_A^2 \omega_A^2} \right\} P, \end{aligned} \quad (10)$$

$$\frac{dP}{d\tau} = -i\delta_A^2 \rho_0 |\Delta_A| \operatorname{sign}(\Omega_r) [-\Lambda_A + i \operatorname{sign}(\Delta_A \Omega_r) \tau] \xi_x,$$

where  $\Lambda_A = 2\omega_A \omega_i / (\delta_A |\Delta_A|)$ . Hence, in the zeroth order, the total pressure perturbation  $P$  is a conserved quantity across the resonance layer. Hence the analytical solutions for  $\xi_x$  and  $P$  inside the dissipative layer around the Alfvén resonance can be found in the following form (Tirry & Goossens 1996):

$$\begin{aligned} \xi_x(\tau) &= - \left[ \frac{\delta_A (\omega_A^2 - \omega_S^2) \tau}{\rho_0 v_A^2 \omega_A^2} + \frac{k_y^2 G_A(\tau)}{\rho_0 \Delta_A} \right] C_A + \mathcal{K}_1, \\ P(\tau) &= C_A, \end{aligned} \quad (11)$$

where

$$G_A(\tau) = \int_0^\infty \left[ e^{iu \operatorname{sign}(\Delta_A \Omega_r) \tau - \Lambda_A u} - 1 \right] e^{-u^3/3} \frac{du}{u},$$

$C_A$  and  $\mathcal{K}_1$  are constants of integration.

In the case of the cusp resonance, an analogous procedure yields the following set of equations (see e.g. Erdélyi 1997)

$$\begin{aligned} & \left[ \frac{d^2}{d\tau^2} + i \operatorname{sign}(\Delta_C \Omega_r) \tau - \Lambda_C \right] \frac{d\xi_x}{d\tau} \\ &= \frac{i \operatorname{sign}(\Omega_r) k_z^2 v_S^4}{\rho_0 |\Delta_C| (v_A^2 + v_S^2)^2} P, \\ & \frac{dP}{d\tau} = -\delta_C \rho_0 \frac{v_A^2 \omega_A^2}{v_A^2 + v_S^2} \xi_x, \end{aligned} \quad (12)$$

where now  $\Omega_r = \omega_r - k_z V = \pm\omega_C$ ,  $\Lambda_C = 2\omega_C \omega_i / (\delta_C |\Delta_C|)$ ,  $\Delta_C \equiv (d/ds)(\Omega^2 - \omega_C^2)$  and

$$\delta_C = \left( \frac{\eta \omega_C}{|\Delta_C|} \right)^{\frac{1}{3}}.$$

with all coefficients evaluated at  $x = x_C$ . According to (12), the total pressure perturbation  $P$  is a conserved quantity across the cusp resonance layer in the zeroth order. Hence the analytical solutions for  $\xi_x$  and  $P$  inside the dissipative layer embracing the cusp resonance are given by :

$$\begin{aligned}\xi_x(\tau) &= -\frac{k_z^2 v_S^4 G_C(\tau)}{\rho_0 \Delta_C (v_S^2 + v_A^2)^2} C_C + \mathcal{K}_2, \\ P(\tau) &= C_C,\end{aligned}\quad (13)$$

where

$$G_C(\tau) = \int_0^\infty \left[ e^{iu \text{sign}(\Delta_C \Omega) \tau - \Lambda_C u} - 1 \right] e^{-u^3/3} \frac{du}{u},$$

$C_C$  and  $\mathcal{K}_2$  are constants of integration.

## 5. The numerical procedure

In the two outer regions of the sharp interface model, i.e. the two semi-infinite homogeneous regions, the solutions for  $\xi_x$  and  $P$  can be found analytically. However in the nonuniform intermediate region, the Eqs. (7) have to be integrated numerically. Application of the continuity condition for  $\xi_x$  and  $P$  at  $x = 0$  and  $x = L$  finally yields the dispersion relation.

Since we are primarily interested in localized surface type eigenmodes, with evanescent amplitudes in both homogeneous regions to the left and the right of the interface, the related oscillation frequencies should lie in the intervals :

$$\omega_{II}(-\infty) > \Omega_r > \omega_I(-\infty) \quad \text{or} \quad \omega_C(-\infty) > \Omega_r$$

and

$$\omega_{II}(+\infty) > \omega_r > \omega_I(+\infty) \quad \text{or} \quad \omega_C(+\infty) > \omega_r.$$

The analytical evanescent solution of (7) valid for  $x < 0$  is simply

$$P(x) = Ae^{\kappa_1 x} \quad \text{and} \quad \xi_x(x) = A \frac{\kappa_1}{C_2(-\infty)} e^{\kappa_1 x} \quad (14)$$

where  $\kappa_1 = \sqrt{-C_1(-\infty)C_2(-\infty)/D(-\infty)}$  and  $A$  is an arbitrarily complex factor. Analogous, the analytical solution for  $x > L$  is given by

$$P(x) = Be^{-\kappa_2 x} \quad \text{and} \quad \xi_x(x) = B \frac{-\kappa_2}{C_2(+\infty)} e^{-\kappa_2 x} \quad (15)$$

where  $\kappa_2 = \sqrt{-C_1(+\infty)C_2(+\infty)/D(+\infty)}$  and  $B$  is an arbitrarily complex factor.

Thus the procedure for solving the eigenvalue problem for the MHD surface modes on the sharp interface is a shooting method from  $x = 0$  to  $x = L$ . Starting at  $x = 0$  with the evanescent analytical solution for the homogeneous region to the left of the interface, we numerically integrate the ideal MHD Eqs. (7). If a resonance is encountered during the calculations, then the dissipative solutions (11) or (13) are applied continuously between the endpoints  $x_{A,C} \pm 5\delta_{A,C}$  of the corresponding dissipative layer. After having passed through the dissipative layer the computations return to the ideal Eqs. (7) until the final point  $x = L$  is reached. Application of the continuity condition for  $\xi_x$  and  $P$  at  $x = L$  yields thus the dispersion relation which has to be solved for  $\omega$  with prescribed  $k_y$ ,  $k_z$  and  $V$ .

## 6. Results

In this section we present the spectrum of the MHD surface waves on a single interface as a function of the velocity shear. We resolve the spectrum for the plasma  $\beta$  parameter equal to zero with and without a nonuniform transition layer. We restricted the calculations to  $\beta = 0$ . This simplifies the picture of the spectrum of the surface modes as function of the velocity shear, since by putting  $\beta = 0$  the slow MHD surface mode is excluded from the model. In the presentation of the results  $\theta$  is defined as the angle of propagation with respect to the magnetic field, i.e.  $k_z = k \cos(\theta)$  and  $k_y = k \sin(\theta)$ . The calculations are performed with  $v_{A1} = 5$  and  $v_{A2} = 1$ .

### 6.1. $\beta = 0$ ; $L = 0$

When  $\beta = 0$ , the slow surface mode is excluded from the configuration, whereas the fast surface mode only exists for a propagation angle  $\theta$  different from  $0^\circ$  and  $90^\circ$ . Since the interface is a true discontinuity, there is no Alfvén continuum so that the surface mode cannot be subject to resonant absorption. Any change in the eigenfrequency is due to the presence of the velocity shear.

In Fig. 2 we have plotted the oscillation frequency of the two fast surface modes for two different angles of propagation  $\theta = 25^\circ, 75^\circ$  (Fig. 2a, Fig. 2b) together with the imaginary part of the eigenfrequency (Fig. 2c, Fig. 2d) as function of the velocity shear  $V$ . The surface mode with positive frequency is a "forward" propagating wave, while the mode with negative frequency is a "backward" propagating wave. The figures clearly show that when the oscillation frequencies of the "forward" and "backward" propagating fast surface modes merge for increasing velocity shear  $V$ , the interface becomes unstable. Hence the merging point indicates the threshold for Kelvin-Helmholtz instability.

### 6.2. $\beta = 0$ ; $L = 0.1$

When we introduce a nonuniform layer, the surface modes with oscillation frequency within the range of the Alfvén continuum resonantly couple to localized Alfvén waves, and, in absence of a velocity shear, they are damped due to the resonant wave excitation.

In Fig. 3a and Fig. 3b we plotted again the oscillation frequencies of the "forward" and "backward" propagating surface modes as function of the velocity shear. In these figures we also indicated the upper and lower bounds of the Alfvén continua  $[-\omega_{A1} + k_z V, -\omega_{A2} + k_z V]$  and  $[\omega_{A2} + k_z V, \omega_{A1} + k_z V]$  which are Doppler shifted due to the presence of the mass flow in the nonuniform layer.

In Fig. 3c and Fig. 3d the corresponding imaginary parts of the eigenfrequencies are plotted as function of the velocity shear  $V$ . For  $V = 0$  both surface modes have their characteristic frequency within the range of the Alfvén continuum (see Figs. 3a and 3b) and hence are damped due to resonant absorption. However when  $V$  is increased, the oscillation fre-

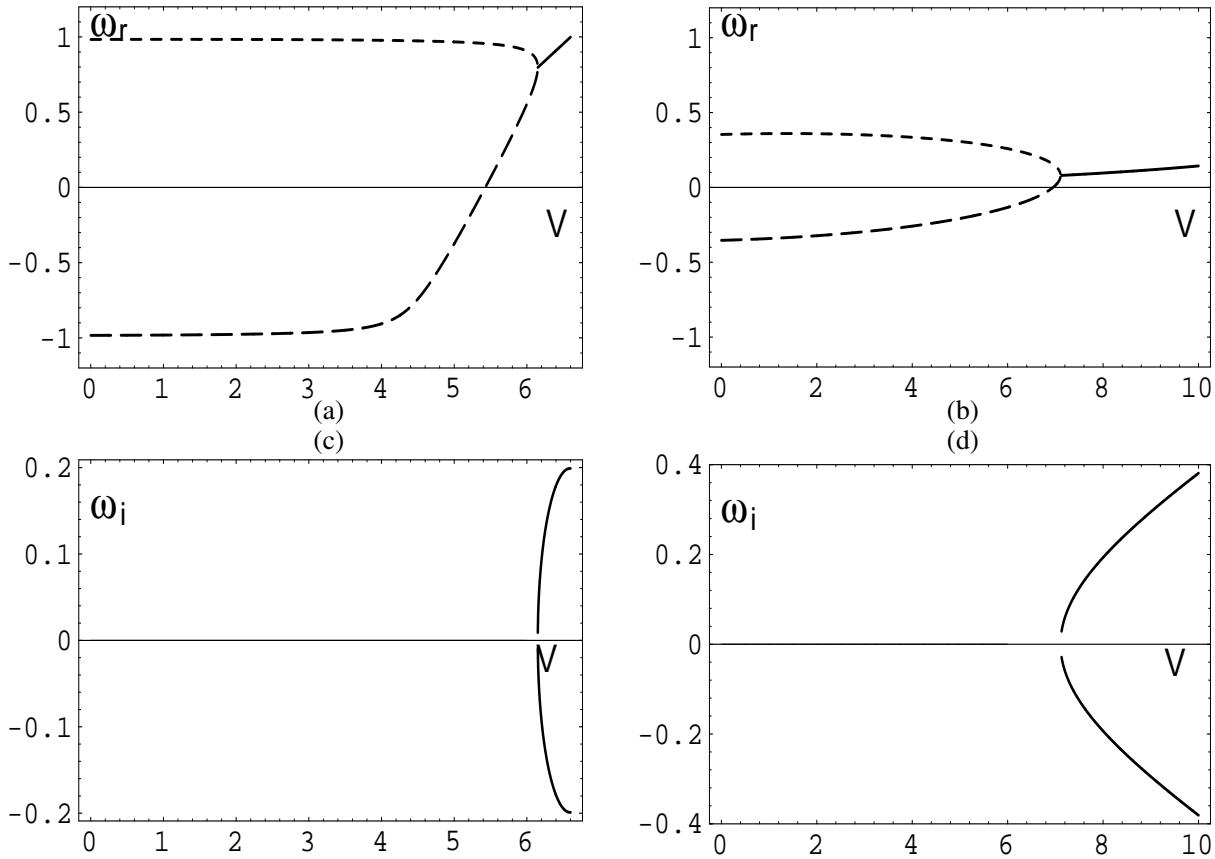


**Fig. 2.** **a** the oscillation frequency of the fast surface modes as function of the velocity shear  $V$  for  $\theta = 25^\circ$  **b** the oscillation frequency of the fast surface modes as function of the velocity shear  $V$  for  $\theta = 75^\circ$  —bf **c** the imaginary part of the frequency of the fast surface modes as function of the velocity shear  $V$  for  $\theta = 25^\circ$  **d** the imaginary part of the frequency of the fast surface modes as a function of the velocity shear  $V$  for  $\theta = 75^\circ$  ( $L = 0$ ).

quency of the "forward" propagating surface mode shifts out of the Doppler shifted upper Alfvén continuum and the mode becomes undamped, whereas the oscillation frequency of the "backward" propagating surface mode remains for a larger interval for  $V$  in the Doppler shifted continuum of "backward" propagating Alfvén modes. In first instance the damping rate increases, reaching a maximum damping rate and then decreases again towards zero at the velocity shear for which the oscillation frequency shifts also out of the Doppler shifted Alfvén continuum.

The most interesting feature in the spectrum appears when the oscillation frequency of the "forward" propagating surface mode shifts into the Doppler shifted continuum of the "backward" propagating Alfvén modes : as long as the oscillation frequency of the "forward" propagating surface mode lies within the range of the Doppler shifted continuum of "backward" propagating Alfvén modes, the surface mode is unstable, i.e.  $\omega_i > 0$ .

Physically this means that the flow acts at the resonant layer as a source of energy from which the surface mode gains energy. From a mathematical point of view, the reason lies in the fact that  $\text{sign}(\Omega) < 0$ , which causes the jump in the Poynting flux across the resonant surface to be negative. The  $x$ -component of the modal energy flux, averaged over the oscillation period, as

seen by an observer fixed relative to some constant flow (which may be taken as the plasma flow  $V$ ) is given by (see e.g. Adam 1978)

$$\begin{aligned} S_x(x, k_y, k_z; \omega) &\approx \frac{1}{2} \text{Re}(P^* \frac{\partial \xi_x}{\partial t}) e^{2\omega_i t} \\ &\approx \frac{1}{2} \text{Re}(-i\omega_r P^* \xi_x) e^{2\omega_i t}, \end{aligned}$$

where the asterisk denotes the complex conjugate. Note that the modal energy flux, averaged over the oscillation period, exponentially increases or decreases depending on the overstability or damping of the mode. With the analytical solution (11) inside the dissipative resonance layer, we can calculate the jump in the energy flux across the dissipative layer as :

$$\begin{aligned} [S_x] &= S_x(x_A - 5\delta_A) - S_x(x_A + 5\delta_A) \\ &\approx \frac{\omega_r C_A^2 k_y^2}{2\rho\Delta} \text{Re}[iG_A(-5) - iG_A(5)] e^{2\omega_i t}. \end{aligned}$$

Using the asymptotic expansion of the function  $G_A(\tau)$  as  $\tau \rightarrow \pm\infty$  (see e.g. Goossens, Ruderman, & Hollweg 1995),

$$\text{Im}(G_A(\tau)) \sim \pm \text{sign}(\Delta\Omega_r) \frac{\pi}{2} \quad \text{as } \tau \rightarrow \pm\infty,$$

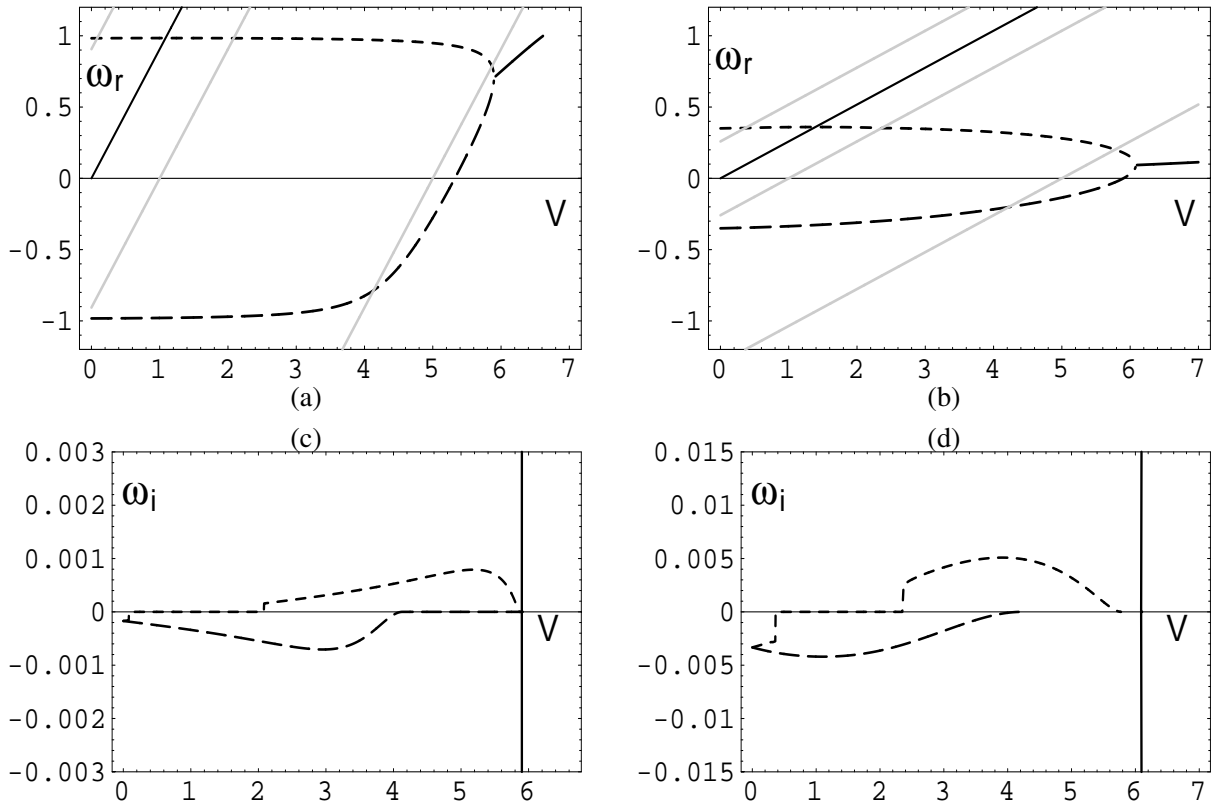


**Fig. 3.** **a** the oscillation frequency of the fast surface modes as a function of the velocity shear  $V$  for  $\theta = 25^\circ$  **b** the oscillation frequency of the fast surface modes as a function of the velocity shear  $V$  for  $\theta = 75^\circ$  **c** the imaginary part of the frequency of the fast surface modes as a function of the velocity shear  $V$  for  $\theta = 25^\circ$  **d** the imaginary part of the frequency of the fast surface modes as a function of the velocity shear  $V$  for  $\theta = 75^\circ$  ( $L = 0.1$ ). The gray lines indicate the upper and lower boundaries of the Doppler shifted Alfvén continua. The full black line stands for  $\omega_r = k_z V$ .

we can reduce the jump in the modal energy flux across the dissipative resonance layer approximately to

$$[S_x] \approx \text{sign}(\Omega_r) \frac{\omega C_A^2 k_y^2}{2\rho|\Delta|} \pi e^{2\omega_i t}. \quad (16)$$

When this jump in energy flux is positive, there is an energy transfer from the fast surface mode in the Alfvén resonance layer and hence the surface mode is damped. However when the jump in energy flux across the resonance layer is negative, this means that there is an energy flow from the resonance layer towards the fast surface mode, which is unstable in this case. This happens only when the oscillation frequency of the “forward” propagating surface mode lies in the Doppler shifted continuum of “backward” propagating Alfvén modes. It is easy to check that the formula (16) is consistent with the Fig. 3c and Fig. 3d.

When the oscillation frequencies of both the “forward” and “backward” propagating surface modes shift out of the lower Doppler shifted Alfvén continuum, they merge leading to Kelvin-Helmholz instability.

## 7. Negative energy waves

To illustrate the correspondence between the overstabilities found here and the negative energy waves, we replace the inhomogeneous transition layer in our model, as described by

Fig. 1, by a tangential discontinuity. For the present discussion, it is also instructive to redraw Fig. 2b (e.g.  $\theta = 75^\circ$ ) in the reference frame in which the region at the left of the discontinuity is static and the region at the right has a mass flow  $-V$ . For  $\beta = 0$ , the dispersion relation in this reference frame is for the two surface modes

$$F(\omega, k_y, k_z) = \frac{\lambda_1}{\rho_1(\Omega_1^2 - \omega_{A1}^2)} + \frac{\lambda_2}{\rho_2(\Omega_2^2 - \omega_{A2}^2)} = 0, \quad (17)$$

where

$$\lambda_i = \sqrt{-\frac{\Omega_i^2 - \omega_{Ai}^2 - v_{Ai}^2 k_y^2}{v_{Ai}^2}}, \quad i = 1, 2,$$

$$\Omega_1 = \omega,$$

$$\Omega_2 = \omega + k_z V.$$

Following Cairns (1979), a wave mode is a negative energy wave when

$$\sigma \omega \frac{\partial F}{\partial \omega} < 0. \quad (18)$$

The coefficient  $\sigma$  has to be taken either 1 or -1 so that in the case of absence of a flow the energy of the modes is positive. After

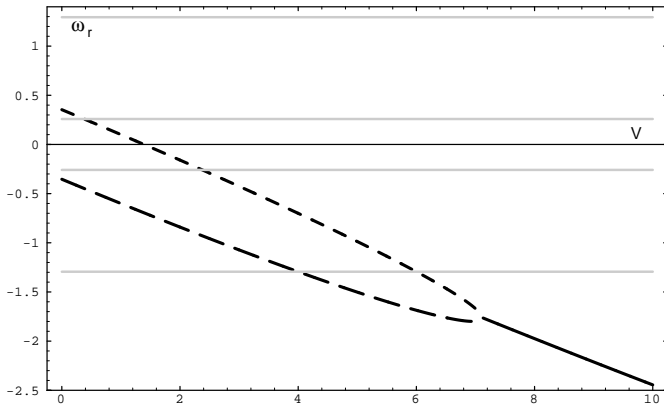


**Fig. 4.** The redraw of Fig. 2b in the reference frame in which the region at the left of the discontinuity is static. The gray lines indicate the upper and lower boundaries of the Alfvén continua.

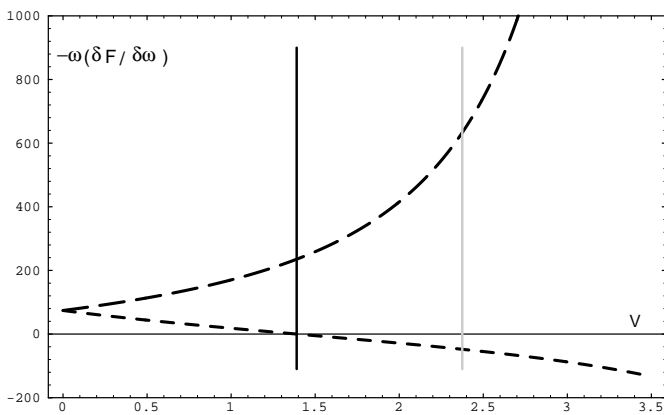


**Fig. 5.**  $-\omega\partial F/\partial\omega$  as function of velocity shear for the eigenfrequencies of the surface modes corresponding to the upper branch and lower branch of Fig. 4. The vertical black line indicates the critical velocity  $V_c$  whereas the vertical gray line indicates the velocity shear for which the eigenfrequency of the negative energy wave enters the lower Alfvén continuum.

some algebra, we obtain for the inequality (18)

$$-\sigma\omega\left[\frac{\omega - k_z V}{\lambda_1((\omega - k_z V)^2 - \omega_{A1}^2)} + \frac{2\lambda_1(\omega - k_z V)}{\rho_1(\omega - k_z V)^2 - \omega_{A1}^2}\right. \\ \left. + \frac{\omega}{\lambda_2(\omega^2 - \omega_{A2}^2)} + \frac{2\lambda_2\omega}{\rho_2(\omega^2 - \omega_{A2}^2)^2}\right] < 0. \quad (19)$$

Using the values of the eigenfrequencies of the two surface modes in Fig. 4 in absence of a velocity shear, we conclude that  $\sigma$  has to be  $-1$ .

In Fig. 5 we plot  $-\omega\partial F/\partial\omega$  as function of velocity shear for the eigenfrequencies of the surface modes corresponding to the upper branch and lower branch of Fig. 4. In this figure we also indicate the critical velocity  $V_c$ , for which the forward propagating surface mode becomes a backward propagating one, with a vertical black line. The velocity shear for which the eigenfrequency corresponding to the upper branch enters the interval  $[-\omega_{A1}, -\omega_{A2}]$ , is indicated with a vertical gray line. Hence in case of a thin nonuniform transition layer the surface mode corresponding to the upper branch, which resonantly couples to a

localized Alfvén continuum mode, is a negative energy wave for  $V > V_c$  and thus becomes unstable due to the presence of dissipation by resonant absorption.

### 8. Summary and discussion

In this paper we investigated how a velocity shear alters the spectrum of the MHD surface modes on a single interface. The single interface is modeled by two semi-infinite uniform regions separated by a nonuniform layer. Due to the presence of nonuniformity a surface mode with characteristic frequency within the range of one of the continuous spectra (associated with the nonuniform layer) may resonantly couple to localized Alfvén and/or slow continuum modes.

To illustrate the combined effect of the velocity shear and the resonant absorption process on the spectrum of the MHD surface modes, we considered in a first step a cold plasma ( $\beta = 0$ ), so that the slow waves are absent. This simplifies the picture of the spectrum of the surface modes as function of the velocity shear.

In the case of a true discontinuity or the single interface, we showed that Kelvin-Helmholtz instability occurs when the oscillation frequencies of the "forward" and "backward" propagating surface modes merge for increasing velocity shear. The merging point then indicates the threshold of Kelvin-Helmholtz instability for the single interface.

In the case of a nonuniform layer, the continuous spectra of "forward" and "backward" propagating Alfvén modes are Doppler shifted due to the presence of the mass flow. When the oscillation frequency of the "forward" ("backward") propagating surface mode lies in the continuum of the "forward" ("backward") propagating Alfvén modes, the surface modes are damped due to the resonant wave excitation. However, when the oscillation frequency of the "forward" propagating fast surface mode lies in the frequency range of the "backward" propagating Alfvén waves, which is only possible due to the presence of the velocity shear, the surface mode is unstable, i.e. the surface mode gains energy from the flow at the resonance layer.

In a reference frame moving with the mass flow, it can clearly be seen that whereas the "backward" propagating surface mode is accelerated, the "forward" propagating surface mode is retarded. Hence a sufficiently large flow changes the sign of propagation. In this case this surface mode becomes a negative energy wave when the shear velocity is larger than a certain critical velocity  $V_c$  (determined by the condition  $k_z V = \omega_r$  in Figs. 3a and 3b) which turns out to be much smaller than the threshold for Kelvin-Helmholtz instability. Note that  $V_c < \min(v_A)$ . With the negative energy, we mean the "linear" part that is associated with the linearized equations and that is of course not the total energy (see Ostrovskii et al. 1986).

Ostrovskii et al. (1986) have shown in hydrodynamics that negative energy waves are unstable when dissipation is present. Later on Ryutova (1988), Hollweg et al. (1990) and Ruderman & Goossens (1995) found the same instabilities of negative energy waves in different dissipative systems. The introduction of wave energy dissipation due to either sound-wave radiation, resonant absorption or viscosity makes negative energy waves

unstable. Hence a presence of any dissipation in the system leads to amplification of the wave. The conservation of energy, however, is not violated, because energy moves from the flow into the waves.

The interpretation in terms of negative energy waves can be worked further out analytically when the thickness of the nonuniform transition layer is assumed to be small compared to the wave length of the surface mode (Erdélyi et al. 1998).

The most important feature of this instability is that its threshold velocity is smaller than the threshold velocity for the onset of the Kelvin-Helmholtz instability. In this paper we restricted the calculations to the  $\beta = 0$  case in order to give a clear picture of the nature of the resonant flow instability. In contrast, the analysis of the solutions inside the dissipative (Alfvén and cusp) resonance layer is performed in a general way, so that extension to parametric studies of more complicated configuration is straightforward.

*Acknowledgements.* V.M.Čadež is grateful to the 'Onderzoeksfonds K.U.Leuven' for awarding him with the senior research fellowship F/97/9. R. Erdélyi is grateful to M. Kéray for her encouragement, and he also thanks PPARC (Particle Physics and Astronomy Research Council) of U.K. awarding him financial support.

## References

- Adam, J.A. 1978, Q. Jl Mech. appl. Math. 20, 77  
 Cairns, R.A. 1979, J. Fluid Mech., 92(1), 1  
 Chandrasekhar, S. 1961, Hydrodynamic and Hydromagnetic Stability, Clarendon Press, Oxford  
 Davila, J. 1987, ApJ, 317, 514  
 Doyle, J.G., O'Shea, E., Erdélyi, R., Dere, K.P., Socker, D.G., & Keenan, F.P. 1997, SPh, 173, 243  
 Erdélyi, R., Goossens, M., & Ruderman, M.S. 1995, SPh, 161, 123  
 Erdélyi, R., & Goossens, M. 1996, A&A, 313, 664  
 Erdélyi, R. 1997, SPh, 171, 49  
 Erdélyi, R., et al. 1998, in preparation  
 Goossens, M., Sakurai, T., & Hollweg, J.V. 1992, SPh, 138, 233  
 Goossens, M., Ruderman, M.S., & Hollweg, J.V. 1995, SPh, 157, 75  
 Hollweg, J.V., & Yang, G. 1988, J. Geophys. Res., 93, 5423  
 Hollweg, J.V., Yang, G., Čadež, V.M., & Gaković, B. 1990, ApJ, 349, 335  
 Ionson, J.A. 1978, ApJ, 226, 650  
 Joarder, P.S., Nakariakov, M.V., & Roberts, B. 1997, SPh, 176, 285  
 Lee, M.A., & Roberts, B. 1986, ApJ, 301, 430  
 Ostrovskii, L.A., Rybak, S.A., & Tsimring, L.S. 1986, Sov. Phys. Usp., 29, 1040  
 Rae, I.C., & Roberts, B. 1982, MNRAS, 201, 1171  
 Roberts B. 1981, SPh, 69, 27  
 Ruderman, M.S., & Goossens, M. 1995, J. Plasma Phys., 54(2), 149  
 Ryutova, M.P. 1988, J. Exper. Theoret. Phys. 94, 138  
 Sakurai, T., Goossens, M., & Hollweg, J.V. 1991, SPh, 133, 227  
 Shibata K. et al. 1992, Publ.Astron.Soc.Japan 44, L173  
 Tirry, W.J., & Goossens, M. 1996, ApJ, 471, 501